



MISS ISADORA SERRAGLIO FORTES (Orcid ID : 0000-0002-3260-4242)

PROFESSOR SAULO FERNANDES ANDRADE (Orcid ID : 0000-0003-2873-7939)

DR ALEXANDRE JOSE MACEDO (Orcid ID : 0000-0002-8951-4029)

Article type : Research Article

Corresponding author email id: alexandre.macedo@ufrgs.br

**N<sub>4</sub>-benzyl-N<sub>2</sub>-phenylquinazoline-2,4-diamine compound presents antibacterial and antibiofilm effect against *Staphylococcus aureus* and *Staphylococcus epidermidis***

Sharon Vieira dos Reis<sup>1</sup>, Nicole Sartori Ribeiro<sup>1</sup>, Débora Assumpção Rocha<sup>2</sup>, Isadora Serraglio Fortes<sup>2</sup>, Danielle da Silva Trentin<sup>3</sup>, Saulo Fernandes de Andrade<sup>2</sup>, Alexandre José Macedo<sup>1,2\*</sup>

<sup>1</sup>Centro de Biotecnologia, Universidade Federal do Rio Grande do Sul, Porto Alegre, Rio Grande do Sul, Brazil

<sup>2</sup>Faculdade de Farmácia, Universidade Federal do Rio Grande do Sul, Porto Alegre, Rio Grande do Sul, Brazil

<sup>3</sup>Departamento de Ciências Básicas da Saúde, Programa de Pós-Graduação em Biociências, Universidade Federal de Ciências da Saúde de Porto Alegre (UFCSPA), Porto Alegre, Rio Grande do Sul, Brazil

\* Corresponding author

This article has been accepted for publication and undergone full peer review but has not been through the copyediting, typesetting, pagination and proofreading process, which may lead to differences between this version and the [Version of Record](#). Please cite this article as [doi: 10.1111/CBDD.13745](https://doi.org/10.1111/CBDD.13745)

This article is protected by copyright. All rights reserved

## Abstract

*Staphylococcus aureus* and *Staphylococcus epidermidis* are the main agents involved with implant-related infections. Their ability to adhere to medical devices with subsequent biofilm formation is crucial to the development of these infections. Herein we described the antibacterial and antibiofilm activities of a quinazoline-based compound, N<sub>4</sub>-benzyl-N<sub>2</sub>-phenylquinazoline-2,4-diamine, against both biofilm-forming pathogens. The minimum inhibitory concentrations (MIC) were determined as 25 µM for *S. aureus* and 15 µM for *S. epidermidis*. At sub-MIC concentrations (20 µM for *S. aureus* and 10 µM for *S. epidermidis*), the compound was able to inhibit biofilm formation without interfere with bacterial growth, confirmed by scanning electron microscopy. Moreover, surfaces coated with the quinazoline-based compound were able to prevent bacterial adherence. In addition, this compound presented no toxicity to human red blood cells at highest MIC 25 µM and *in vivo* toxicity assay using *Galleria mellonella* larvae resulted in 82% survival with a high-dose of 500 mg/kg body weight. These features evidence quinazoline-based compound as interesting entities to promising applications in biomedical fields, such as antimicrobial and in anti-infective approaches.

**Key words:** *Staphylococcus aureus*, *Staphylococcus epidermidis*, antibiofilm, antibacterial, coating, quinazoline

It is well known that biofilm formation is an important virulence factor to develop many chronic infections (Koo, 2017), accounting for more than 80% of microbial infections in humans (Davies, 2003). Biofilms are formed by multiple microbial cells attached to a surface or suspended in interfaces, which are organized in a complex tertiary structure embedded in an extracellular matrix of polymeric substances (Blackledge, 2013). Bacteria in biofilm are phenotypically distinct of their planktonic counterparts, especially regarding gene expression and growth rates (Del Pozo, 2017), being more tolerant to clearance by antibiotics and the host immune system (Blackledge, 2013). Since biofilms can serve as reservoirs for bacterial pathogens, leading to persistent infections and allow resistant gene transfer, biofilm-related diseases represent a considerable economic burden, contributing to patient morbidity and increased mortality rates (Del Pozo, 2017).

Medical devices can improve the quality of life and longevity of patients, and are frequently used in almost all fields of medicine for diagnostic and therapeutic procedures. The average rates of infection related to surgical implants are 0.5-5% for joint prosthesis, 7-15% for mechanical and bioprosthetic heart valves, 3.1-7.5% for urinary devices, and 40% for ventricular assist devices (VanEpps, 2016). Biomaterials are prone to be infected during its implantation by microorganisms from patient's skin or from the hands of the surgical or clinical staff, and the infected implants often need to be removed to complete elimination of infection (VanEpps, 2016). *Staphylococcus aureus* and *Staphylococcus epidermidis* account together for two thirds of etiological agents related to implant-associated infections (Campoccia, 2016), evidencing their importance in this type of disease. *S. epidermidis* and *S. aureus* are opportunistic pathogens that only can cause infection in healthy patients when disrupting epithelial barrier (Otto, 2012). Biofilm formation is an essential virulence factor that contributes to establish chronic infections. *S. aureus* biofilm-related infections require intensive care, and infected devices need to be removed more frequently than those infected by *S. epidermidis*.

Due to the difficulty in treating biofilm-related infections, efforts are made to find novel active compounds able to treat or prevent biofilm formation. Quinazolines are an emerging class of compounds, and many appropriate substituted quinazolines have shown a wide range of activities for medication purpose, such as antimalarial, antiviral, anticancer, antifungal, antiprotozoan, anti-inflammatory, besides other biological activities

(Asif, 2014). Quinazoline ring is part of many approved drugs in the market such as prazosin hydrochloride, doxazosine mesylate and terazosine hydrochloride, all of them being used to treat high blood pressure and benign prostatic hyperplasia. Also, there are numerous reports describing antibacterial activity of quinazoline derivatives against both Gram-positive and negative strains (Fleeman, 2017; Jafari, 2016; Van Horn, 2014) . There are still few studies focused on antibiofilm activity of this class of compounds, although they demonstrate its promising potential for this purpose (Bessa, 2016; Bisacchi, 2015; Chandrasekera, 2017; Fleeman, 2017; Kant, 2017; Rasmussen, 2011; Zhang, 2015). In this work we evaluated the antibacterial and antibiofilm activities of a quinazoline-based compound, N<sub>4</sub>-benzyl-N<sub>2</sub>-phenylquinazoline-2,4-diamine, denominated PH100, against *S. aureus* and *S. epidermidis* bacteria.

## Results and Discussion

The antibacterial activity of the substituted quinazoline PH100 (Figure 1A) was firstly assessed by determination of MIC and MBC against *S. aureus* ATCC 25904 and *S. epidermidis* ATCC 35984 after 24 h incubation (Table S1). The MIC values of PH100 for *S. aureus* and *S. epidermidis* were 25  $\mu$ M and 15  $\mu$ M, and the MBC values were 400  $\mu$ M and 100  $\mu$ M, respectively. The ratios MBC/MIC were 16 for *S. aureus* and 6.7 for *S. epidermidis* (Table S1), which characterize bacteriostatic compounds since those numbers are greater than 4 (Pankey, 2014).

Growth curves for both microorganisms (Figure 1B and C) show that at MIC and higher concentrations of PH100 (25 and 50  $\mu$ M for *S. aureus* and 15, 20 and 25  $\mu$ M for *S. epidermidis*), an initial growth was observed within the first 3-4 h, but it decreased afterwards. However, at sub-inhibitory concentrations (15 and 20  $\mu$ M for *S. aureus* and 5 and 10  $\mu$ M for *S. epidermidis*), PH100 had no statistically significant inhibitory effect on bacterial growth when compared with the vehicle control during the stationary growth phase. The bacteriostatic profile of PH100 against these microorganisms was also noticed through growth curves, where both bacteria were able to restore growth after 24 h incubation when treated at MIC. Trentin *et al.* (2013) also observed this pattern on kinetic analysis of antibacterial activity with plant extracts, which demonstrated to be bacteriostatic against *Pseudomonas aeruginosa* (Trentin, 2013).

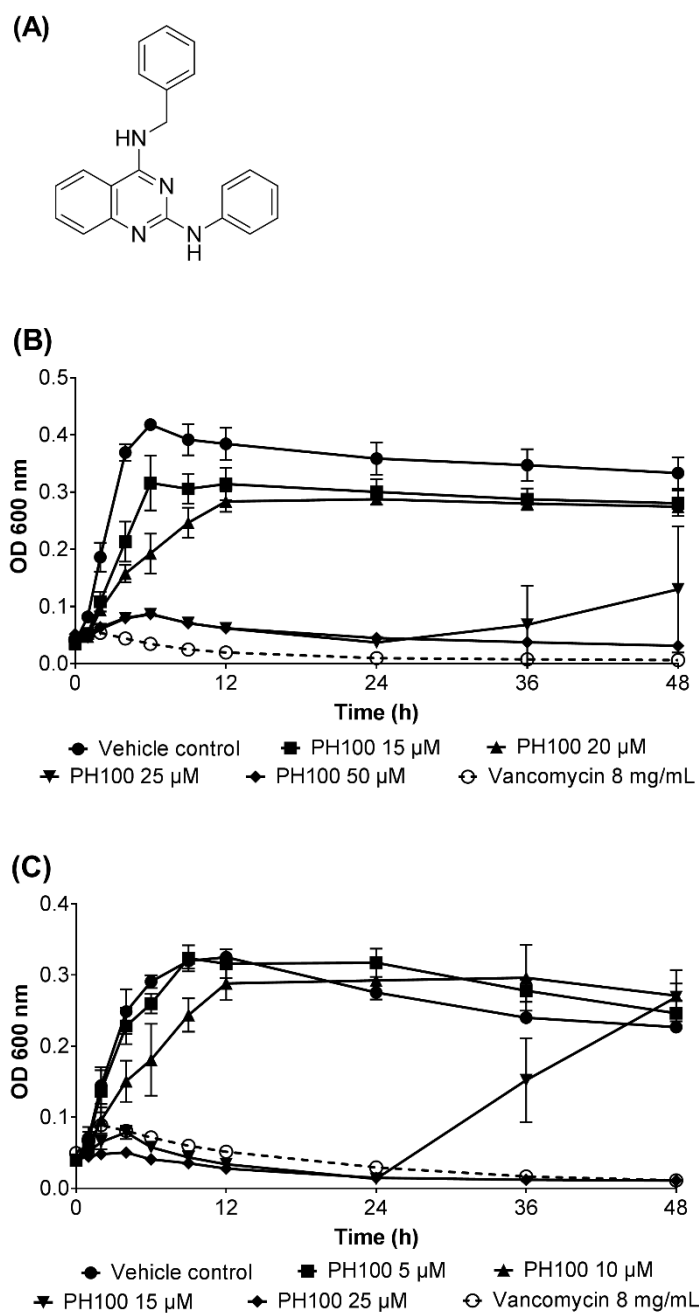


**Figure 1.** Bacterial kinetic growth curve in presence of  $N_4$ -benzyl- $N_2$ -phenylquinazoline-2,4-diamine (PH100) structure (A) of *S. aureus* (B) and *S. epidermidis* (C). Bacterial growth evaluated at different concentrations of PH100 during 48 h incubation. DMSO (2%) was used as vehicle control, and vancomycin was used as bactericide control. Error bars indicate the standard deviations of three independent experiments.

Once biofilms are established, they are difficult to eradicate due to their inherent reduced susceptibility to antibacterial, often resulting in failure of antimicrobial treatment and mechanical removal requirement of the biofilm (Del POzo, 2017). Bacterial adhesion on medical devices surfaces is the first and crucial step for established device-related infections (Campoccia, 2006). Therefore, prevention of bacterial attachment still represents the best approach to suppress infectious process development. As an attempt to eliminate or reduce bacterial adhesion and biofilm formation, intensive efforts have been focused on the development of antibacterial surfaces by application of coatings, modification or alteration its architecture (Hasan, 2013). In this sense, numerous works focus on coating surfaces with one or two antimicrobials or entrapping these chemicals within the material, aiming to obtain medical devices with different antimicrobial spectra and span of the antimicrobial effect (Francolini, 2010).

Treatments with sub-inhibitory concentrations of PH100 significantly reduced *S. aureus* and *S. epidermidis* biofilm formation (Figure 2A and B, respectively). The production of biofilm biomass was reduced approximately 51% when *S. aureus* was treated with 20  $\mu\text{M}$  PH100, and 94% when *S. epidermidis* was treated with 10  $\mu\text{M}$  PH100, in comparison to the untreated control. Interestingly, these concentrations under MIC had no impact on bacterial growth rates, as demonstrated by kinetics curve and confirmed by concomitant spectrophotometric evaluation at OD<sub>600 nm</sub> during biofilm assays (Figure 1 and 2). As expected, treatments at MIC and upper concentrations, as well as vancomycin, were able to inhibit biofilm formation by impairing bacterial growth (Figure 2). Both strains of *S. aureus* and *S. epidermidis* tested are strong biofilm formers.

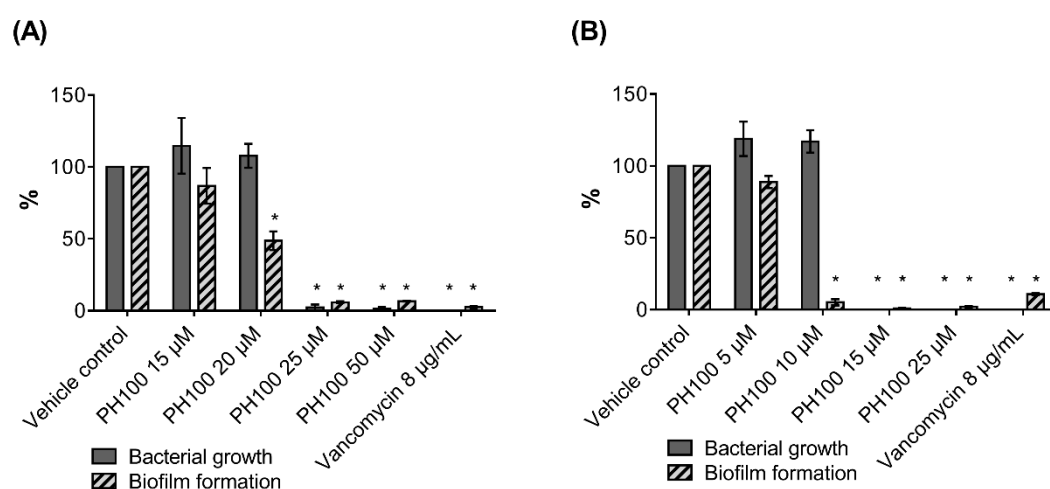


**Figure 2.** Evaluation of *S. aureus* (A) and *S. epidermidis* (B) biofilm formation and bacterial growth in the presence of PH100. Biofilm biomass was quantified using crystal violet staining and bacterial growth was assessed by spectrophotometric measurements at 600 nm. Results are presented as percentage compared to vehicle controls, which are considered as 100% of bacterial growth and biofilm formation. The error bars indicate the standard deviations of three experiments. \* $p < 0.01$  vs. untreated vehicle control groups.

An ideal approach to fight biofilms would be the prevention of bacterial adhesion or the interruption of the regulatory systems involved in biofilm formation and maintenance, without killing bacteria, avoiding higher pressure for the selection of resistant bacterial population (Blackledge, 2013). In this regard, PH100 at sub-inhibitory concentrations could be a possible candidate for this purpose. It is important to mention that many studies have demonstrated that some antibacterials, such as kanamycin, erythromycin and azithromycin, when used at sub-MIC concentrations, can enhance biofilm formation (Jones, 2013; Kuehl, 2009; Wang, 2010), evidencing that inappropriate antibacterial choice or usage would improve bacterial biofilm formation during infectious disease, leading to a worsening clinical outcome. Otherwise, the compound evaluated in this study did not stimulate this response in any strain tested and can be useful as antibacterial on higher concentrations or antibiofilm on sub-MIC concentrations. The significant reduction in *S. aureus* and *S. epidermidis* biofilm development observed in crystal violet assay when cells were treated those sub-MIC concentrations of PH100 (Figure 2) was confirmed by scanning electron microscopy images (Figure 3). Several bacterial aggregates can be visualized in control sample, which did not receive PH100 treatment (Figure 3A and D). *S. epidermidis* formed thicker biofilm than *S. aureus*, as observed in the controls. As expected, in the presence of PH100, the adhesion of bacterial cells decreased in number and in size of clusters in concentration-dependent manner (Figure 3B, C, E and F). Even at the lowest concentration tested (PH100 15  $\mu\text{M}$  for *S. aureus*, and PH100 5  $\mu\text{M}$  for *S. epidermidis*), a reduction of adhered cells can be observed for both bacteria (Figure 3B and E), however this effect was not observed using only the crystal violet technique.

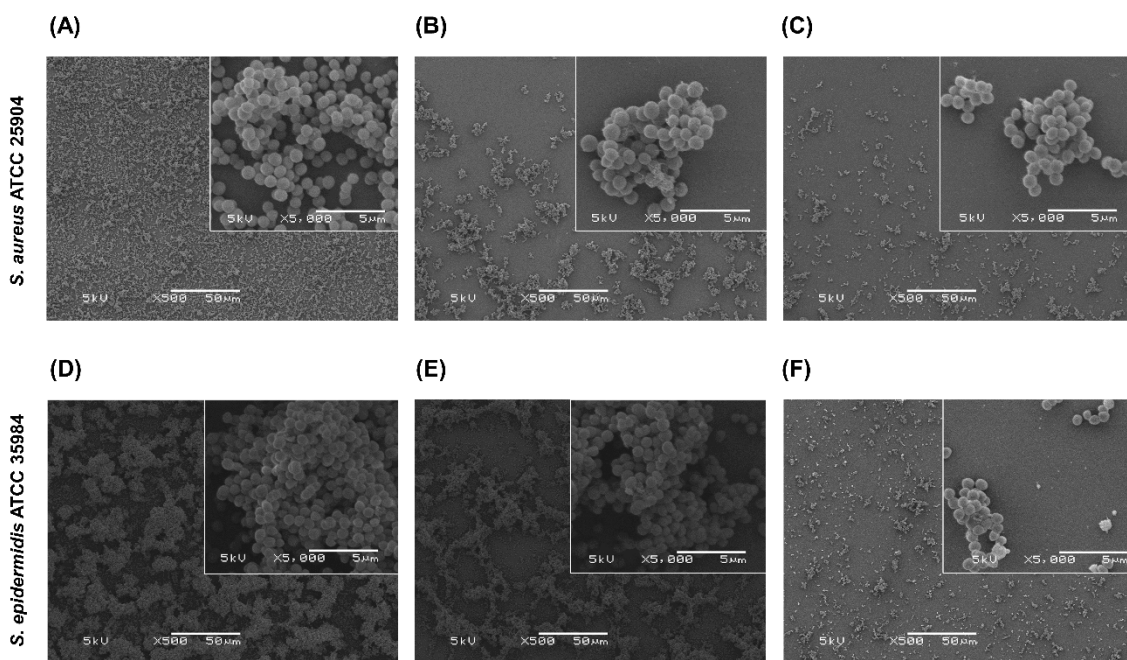


**Figure 3.** SEM images of *S. aureus* and *S. epidermidis* biofilm in the absence or presence of sub-MIC concentrations of PH100. *S. aureus* biofilms formed in the presence of 2% DMSO vehicle (A); *S. aureus* biofilms formed in the presence of PH100 15  $\mu\text{M}$  (B), and in the presence of PH100 20  $\mu\text{M}$  (C); *S. epidermidis* formed in the presence of 2% DMSO vehicle (D); *S. epidermidis* biofilms formed in the presence of PH100 5  $\mu\text{M}$  (E), and in the presence of PH100 10  $\mu\text{M}$  (F). Scale bars: 50  $\mu\text{m}$  at the main images, 5  $\mu\text{m}$  at the inserts.

Based on these results, we prepared PH100-coated surfaces by using spin-coating technique, in order to verify its ability to prevent bacterial adherence and biofilm growth. SEM images of PH100-coated surface samples showed that acetone-treated surface (vehicle control) allowed bacteria attachment and biofilm development by *S. aureus* (Figure 4A) and *S. epidermidis* (Figure 4C). As previously observed in SEM, *S. epidermidis* formed thicker biofilms than *S. aureus*, presenting many aggregated cells in the control condition. However, a lower number of bacterial attached cells were presented on PH100-treated surface in comparison to acetone-treated surface for both bacteria, which means that the adhesion was inhibited in PH100- surface presence (Figure 4B and D), with no bacterial clusters observed. Despite of these results, this assay did not measure the bacterial viability, therefore this effect could be reached by

action on bacteria growth or on virulence factor related to attachment. The compound has low aqueous solubility (Van Horn, 2014), which may contribute to a strong interaction with the Permanox™ material used as model surface, avoiding its removal even after several washes. This feature might be important not only for a long maintenance of biofilm inhibition, but also to prevent the compound detachment from the material surface.

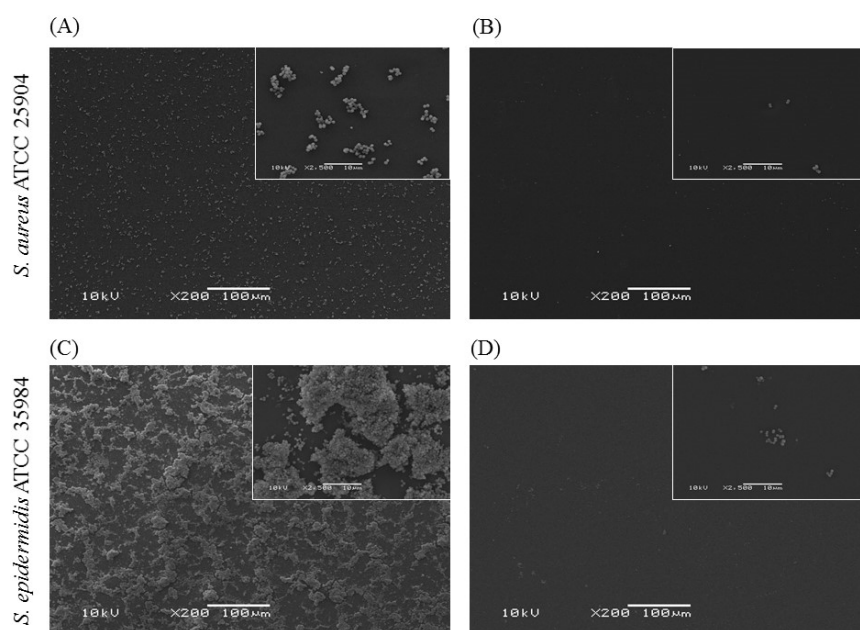


**Figure 4.** SEM images of *S. aureus* and *S. epidermidis* biofilm formation on PH100-coated surface. *S. aureus* (A) and *S. epidermidis* (C) acetone-treated surface used as vehicle control; *S. aureus* (B) and *S. epidermidis* (D) biofilm in PH100-coated surface. Scale bars: 100 μm at the main images, 10 μm at the inserts.

In order to investigate the potential toxicity of PH100, a preliminary study using human red blood cells and an invertebrate host model were carried out. Hemolytic effect in human red blood cells was conducted as indicative of cytotoxicity (Figure S1). For this, triton X-100 was used as a positive control and was considered to cause 100% hemolysis while vehicle (2% DMSO) was used as negative control and considered to cause no hemolysis. PH100 concentrations, ranging from 10 to 25 μM, did not present a significant hemolytic activity. Only the highest concentration tested (50 μM) presented low (approximately 3.5%), but significant hemolysis when compared to negative control. Fleeman *et al.* (2017) also tested the hemolytic capacity of six substituted quinazolines

using whole human blood. They registered average hemolysis below 1% at 10  $\mu$ M, which was in accordance with the present study. Additionally, *Galleria mellonella* larvae was used as an alternative invertebrate model to evaluate *in vivo* toxicity of PH100. This model has been used over the last years for toxicity evaluation, demonstrating data correlation to cell culture and mammalian models (Maguire, 2016; Megaw, 2015; Sardi, 2017). A single high-dose of 500 mg/kg of larvae was tested in groups of 10 larvae. Since PH100 was only soluble in DMSO, it was injected at a final volume of 1  $\mu$ L to larvae hemocoel. As control, 1  $\mu$ L of DMSO was administered. All larvae groups were incubated at 37 °C during 5 days and survival was evaluated at each 24 h through touch stimuli. PH100-treated group presented approximately 82% survival (Table S2), which was not statistically different from the negative control, indicating that LD<sub>50</sub> for PH100 (minimum dose able to kill 50% of the larvae over time) is higher than dose of 500 mg/kg.

In conclusion, this work presented a promising quinazoline compound displaying both antibiofilm and antibacterial activity, depending on employed concentration. PH100 presented low toxicity and was able to inhibit biofilm formation under sub-inhibitory concentrations without interfering with bacterial growth. The bioactivity of PH100 is kept even when adsorbed in a material surface since PH100 avoids bacterial adhesion, leading to the generation of an anti-staphylococcal surface. Since staphylococci comprise the major cause of implant-related biofilms, PH100 would have potential uses as anti-infective strategy such as for the coating of medical devices surfaces.

## Methods

### *PH100 (N<sup>4</sup>-benzyl-N<sup>2</sup>-phenylquinazoline-2,4-diamine) synthesis*

PH100 is a quinazoline derivative, denominated N<sup>4</sup>-benzyl-N<sup>2</sup>-phenylquinazoline-2,4-diamine. The synthesis procedure is represented in Figure S2. First, to a stirred solution of 2,4-dichloroquinazoline **1** (2.51 mmol) in THF/H<sub>2</sub>O (3:1) (15 mL), were added sodium acetate (2.76 mmol) and benzilamine (2.76 mmol). The mixture was stirred for 6 h at 65 °C. After, it was cooled and diluted with ethyl acetate (40 mL) and water (40 mL) and the organic layer was washed with water (2x40 mL), dried over Na<sub>2</sub>SO<sub>4</sub>, filtered and concentrated under reduced pressure. The residue was purified by silica gel column chromatography eluting with cyclohexane: ethyl acetate (85:15) to give **2** in 62% yield

which was used immediately in the next step. To a solution of **2** (0.0926 mmol) in ethanol (0.5 mL), aniline was added (0.139 mmol). The correspondent mixture was stirred for 3 h at 120 °C. After, the mixture was cooled, diluted with ethyl acetate (20 mL) and washed with a solution of sodium bicarbonate 10% (p/v) (20 mL) and water (20 mL). The organic layer was dried with Na<sub>2</sub>SO<sub>4</sub> anhydrous, filtered and concentrated under reduced pressure. The residue was purified by silica gel column chromatography eluting with cyclohexane: ethyl acetate (7:3) to give PH100 as a yellow solid in 81% yield. After this purification we proceeded with spectroscopy analyses using infrared (IR), <sup>1</sup>H and <sup>13</sup>C Nuclear Magnetic Resonance (NMR) and mass spectrometry (Figures and description available in the supporting information) to verify identity and purity of PH100 which is in accordance with the work of Van Horn (2014)<sup>25</sup>. M.p. 142-145 °C. IR ( $\nu$  /cm<sup>-1</sup>): 3431, 3027, 1568, 1485, 1415, 1326. <sup>1</sup>H NMR (400 MHz, DMSO-*d*<sub>6</sub>)  $\delta$  9.02 (s, 1H), 8.68 (t, 1H, *J* = 5.4 Hz), 8.16 (d, 1H, *J* = 8.0 Hz), 7.84 - 7.82 (m, 2H), 7.60 (t, 1H, *J* = 8.0 Hz), 7.44-7.40 (m, 3H), 7.33 (t, 2H, *J* = 7.4 Hz), 7.25- 7.18 (m, 4H), 6.86 (t, 1H, *J* = 7.2 Hz), 4.83 (d, 2H, *J* = 5.4 Hz). <sup>13</sup>C NMR (100 MHz, DMSO-*d*<sub>6</sub>)  $\delta$  160.1, 156.9, 151.4, 141.4, 139.7, 132.6, 128.3, 127.1, 126.7, 125.3, 122.8, 121.5, 120.4, 118.5, 111.6, 43.5. HRMS (*m/z*): [MH<sup>+</sup>] calc for C<sub>21</sub>H<sub>19</sub>N<sub>4</sub>, 326,1604; found, 327,1604 (Fig. S3 – S5).

#### *Bacterial strains and culture conditions*

*Staphylococcus aureus* ATCC 25904 and *Staphylococcus epidermidis* ATCC 35984 were grown in Muller Hinton (MH) agar (Himedia, India) overnight at 37 °C. Bacterial suspensions used in the assays were prepared in sterile 0.9% NaCl at optical density at 600 nm (OD<sub>600</sub>) of 0.150 (corresponding to a concentration of 3x10<sup>8</sup> UFC/mL and 1 McFarland scale). PH100 stock solutions were prepared in DMSO (Sigma-Aldrich, USA). As routine of the laboratory the quality control of the strains were performed by disk diffusion following procedures and interpretation criteria indicated by CLSI. Particularly in this case, we used the gram-positive reference bacteria *S. aureus* ATCC 25923 and all parameters fitted with CLSI (2018).

#### *Minimum Inhibitory Concentration (MIC) and Minimum Bactericidal Concentration (MBC) determination*

The MIC was evaluated as described by Trentin *et al.* (2013) with slight modifications. Final concentrations ranging from 5 to 400  $\mu\text{M}$  of PH100 were evaluated in 96-well microtiter plates (Costar 3599, Corning, Inc., USA). Each well was inoculated with 80  $\mu\text{L}$  of bacterial suspension, 40  $\mu\text{L}$  of TSB (Oxoid Ltd., England) (supplemented with 1% glucose for *S. aureus*), 76  $\mu\text{L}$  of deionized water and 4  $\mu\text{L}$  of PH100 in DMSO. Wells without addition of bacteria were used as negative controls. The plates were incubated statically at 37 °C for 24 h, and bacterial growth was evaluated by measuring turbidity at 600 nm. MIC values were reported as the lowest concentration of PH100 at which no increase in  $\text{OD}_{600}$  measure was observed after 24 h incubation. The MBC was determined by dropping 10  $\mu\text{L}$  of bacterial culture from wells with concentrations greater or equal to the MIC value on MH agar plates. The agar plates were incubated overnight at 37 °C and MBC was defined as the concentration at which no bacterial colony growth was observed after 24 h incubation.

#### *Antibacterial activity kinetics*

The effect of PH100 on bacterial growth was evaluated at MIC and at concentrations below and above the MIC. The assay was prepared as described for MIC determination.  $\text{OD}_{600}$  was measured at 0, 1, 2, 4, 6, 9, 12, 24, 36 and 48 hours of incubation at 37 °C. Controls were prepared with DMSO replacing PH100 treatment. Vancomycin (8  $\mu\text{g}/\text{mL}$ ) was used as bactericide control.

#### *Biofilm formation assay*

The antibiofilm activity of PH100 was evaluated using the crystal violet assay adapted from Trentin *et al.* (2011). Briefly, 40  $\mu\text{L}$  of TSB (supplemented with 1% glucose for *S. aureus*), 80  $\mu\text{L}$  of bacterial suspension, 76  $\mu\text{L}$  of deionized water and 4  $\mu\text{L}$  of PH100 in DMSO at various concentrations were added to 96-well microtiter plates and incubated for 24 h at 37 °C. After the incubation period, the wells were washed 3 times with sterile saline, heat-fixed at 60 °C for 1 hour, and stained with 0.4% crystal violet for 15 minutes. The plates were washed, the remaining dye were solubilized with 99% ethanol and the absorbance was measured at 570 nm. PH100 was tested at final concentrations ranging from 5 to 50  $\mu\text{M}$ , and it was replaced by DMSO in the untreated control, which represented 100% biofilm formation.

### *Scanning electron microscopy (SEM)*

Biofilms of *S. aureus* ATCC 25904 and *S. epidermidis* ATCC 35984 were formed on pieces of Permanox™ slide (Nalge Nunc International, USA) placed in 96-well microtiter plates, in the same conditions as described for biofilm formation assays. After 24 h incubation at 37 °C, the Permanox™ pieces were washed with sterile saline and fixed with 2.5% glutaraldehyde. The samples were prepared for analysis by washing with 100 mM cacodylate buffer (pH 7.2), dehydrating in increasing concentrations of acetone (10%, 30%, 50%, 70%, 90% and 100%), and drying using the CO<sub>2</sub> critical point technique. The Permanox™ pieces were fixed in aluminum stubs, covered with gold film, and visualized in a JEOL JSM-6060 scanning electron microscope at 5 kV. Sub-inhibitory concentrations of PH100 (15 μM and 20 μM for *S. aureus* and *S. epidermidis*, respectively) were evaluated, and untreated samples were used as controls for biofilm formation.

### *PH100 coated-surface*

The coating surface protocol was adapted from Trentin *et al.* (2015). Briefly, 300 μL of a 4.0 mg ml<sup>-1</sup> P100 solution in 70% aqueous acetone (Merk, Germany) was spin coated on pieces of Permanox™ slide (30 x 25 mm<sup>2</sup>) first with a 500 rpm (5 s) cycle and then accelerated to 5000 rpm for 40 s in a spin coater (Laurell Model WS-650MZ-23NPP/LITE). After this step, the pieces were heat-treated at 80°C for 2 h to fix the compound and remove solvent excess. The slides were sterilized with UV light during 20 minutes, cut in 10 x 25 mm<sup>2</sup> coated pieces and then washed 10 times with sterile saline to analyze compound adhesion. As control, Permanox slides were spin coated with 300 μL of 70% acetone solution and submitted to the same procedures as described above. Samples were then analyzed to evaluate biofilm growth by SEM as described at 2.6 section.

### *Hemolysis assay*

Human venous blood (Universidade Federal do Rio Grande do Sul Ethics Committee under number 1.202.565) was collected in tubes containing EDTA, and centrifuged at 1200 g for 10 min. The supernatant was discarded; the erythrocytes were washed three times with 10 mM phosphate buffer saline (pH 7.4/ 0.9% NaCl) and

resuspended in the same buffer at 3% hematocrit. For hemolytic assay, 500  $\mu$ L of erythrocytes suspension, 480  $\mu$ L of PBS and 20  $\mu$ L of PH100 (final concentration ranging from 10 to 50  $\mu$ M) were incubated for 1 h at 37 °C. The negative control (NC) was prepared replacing treatment by DMSO, and 1% Triton X-100 was used for positive control (PC). The supernatants were collected by centrifugation at 3000 rpm for 5 min, and their hemoglobin content were assessed spectrophotometrically at 540 nm. The percentage of hemolysis was calculated as follows: %Hemolysis= Abs Treatment  $\times$ 100/ Abs PC – Abs NC

#### *In vivo toxicity in Galleria mellonella larvae*

For toxicity assay, groups of ten larvae of *G. mellonella* in the final instar larval stage weighing 225–275 mg were used. Larvae were injected using a 10  $\mu$ L Hamilton syringe via the last right proleg with 500 mg/kg of PH100 diluted in 1  $\mu$ L DMSO. As a control of vehicle, a group of larvae received 1  $\mu$ L DMSO. The larvae were incubated at 37 °C for 5 days and daily the survival was recorded as response to touch stimuli.

#### *Statistical analysis*

These assays were performed at least in triplicate. Data were analyzed using the software GraphPad Prism version 6.01 by two-tailed t test comparing with the untreated controls. A  $p < 0.01$  was considered statistically significant and the results are expressed as mean  $\pm$  standard deviation. Statistical significance in *G. mellonella* survival analyses was determined by the log-rank test (GraphPad Prism 6.01).

#### **Acknowledgments**

We thankfully acknowledge CME/UFRGS for technical assistance in scanning electron microscopy and Viviane Nunes da Silva Anselmo for technical support. This work was supported by FAPERGS-PRONEM (16/2551-0000244-4), MCTI/CNPq (303353/2016-3, 312351/2017-8), Universal/CNPq (443150/2014-1 and 425970/2018-3), CAPES (88887.130212/2017-01). and CAPES (Finance Code 001).

#### **Conflict of Interest**

The authors declare no competing financial interest.

## Data Availability Statement

The data that support the findings of this study are available from the corresponding author upon reasonable request.

## References

Asif, M. (2014). Chemical Characteristics, Synthetic Methods, and Biological Potential of Quinazoline and Quinazolinone Derivatives. *International Journal Medical Chemistry*, 395637. doi:10.1155/2014/395637

Bessa, L. J., Buttachon, S., Dethoup, T., Martins R., Vasconcelos, V., Kijjoa, A., Martins da Costa, P. (2016). Neofiscalin A and fiscalin C are potential novel indole alkaloid alternatives for the treatment of multidrug-resistant Gram-positive bacterial infections. *FEMS Microbiology Letters*, 363, fnw150. doi:10.1093/femsle/fnw150

Bisacchi, G. S. & Manchester, J. I. (2015). A New-Class Antibacterial-Almost. Lessons in Drug Discovery and Development: A Critical Analysis of More than 50 Years of Effort toward ATPase Inhibitors of DNA Gyrase and Topoisomerase IV. *ACS Infectious Disease*, 1, 4–41. doi: 10.1021/id500013t

Blackledge, M. S., Worthington, R. J., Melander, C. (2013). Biologically inspired strategies for combating bacterial biofilms. *Current Opinion Pharmacology*, 13, 699–706. doi:10.1016/j.coph.2013.07.004

Campoccia, D., Montanaro, L., Arciola, C. R. (2006). The significance of infection related to orthopedic devices and issues of antibiotic resistance. *Biomaterials*, 27, 2331–2339. doi:10.1016/j.biomaterials.2005.11.044

Chandrasekera, N. S., Berube, B. J., Shetye, G., Chettiar, S., O'Malley, T., Manning, A., Flint, L., Awasthi, D., Ioerger, T. R., Sacchettini, J., Masquelin, T., Hipskind, P. A., Odingo, J., Parish, T. (2017). Improved Phenoxyalkylbenzimidazoles with Activity against *Mycobacterium tuberculosis* Appear to Target QcrB. *ACS Infectious Disease*, 3,

898–916. doi: 10.1021/acsinfecdis.7b00112

Clinical and Laboratory Standards Institute (CLSI) (2018). M100: Performance Standards for Antimicrobial Susceptibility Testing. 28th ed.

Davies D. (2003). Understanding biofilm resistance to antibacterial agents. *Nature Reviews Drug Discovery*, 2, 114–122. doi:10.1038/nrd1008

Del Pozo, J. L. (2017). Biofilm-related disease. *Expert Review of Anti-infective Therapy*, 1–15. doi:10.1080/14787210.2018.1417036

Fleeman, R., Van Horn, K. S., Barber, M. M., Burda, W. N., Flanigan, D. L., Manetsch, R., Shaw, L. N. (2017). Characterizing the antimicrobial activity of N2,N4-disubstituted quinazoline-2,4-diamines toward multidrug-resistant *Acinetobacter baumannii*. *Antimicrobial Agents Chemotherapy*, 61, 1–11. doi: 10.1128/AAC.00059-17

Francolini I. & Donelli, G. (2010). Prevention and control of biofilm-based medical-device-related infections. *FEMS Immunology Medical Microbiology*, 59, 227–238. doi:10.1111/j.1574-695X.2010.00665.x

Hasan , J., Crawford, R. J., Ivanova , E.P. (2013). Antibacterial surfaces: the quest for a new generation of biomaterials. *Trends Biotechnology*, 31, 295–304. doi:10.1016/j.tibtech.2013.01.017

Jafari, E., Khajouei, M. R., Hassanzadeh, F., Hakimelahi, G. H., Khodarahmi, G. A. (2016). Quinazolinone and quinazoline derivatives: Recent structures with potent antimicrobial and cytotoxic activities. *Research in Pharmaceutical Sciences*, 11, 1–14.

Jones, C., Allsopp, L., Horlick , J., Kulasekara, H., Filloux A. (2013). Subinhibitory concentration of kanamycin induces the *Pseudomonas aeruginosa* type VI secretion system. *PLoS One*, 8, e81132. doi:10.1371/journal.pone.0081132

Kant, S., Asthana, S., Missiakas, D., Pancholi, V. (2017). A novel STK1-targeted small-molecule as an antibiotic resistance breaker against multidrug-resistant *Staphylococcus aureus*. *Scientific Reports*, 7, 5067. doi:10.1038/s41598-017-05314-z

Koo, H., R.N. Allan, Howlin, R. P., Stoodley, P., Hall-stoodley, L. (2017). Targeting microbial biofilms: current and prospective therapeutic strategies. *Nature Reviews Microbiology*, 15, 740–755. doi:10.1038/nrmicro.2017.99

Kuehl, R., Al-Bataineh, S., Gordon, O., Luginbuehl, R., Otto, M., Textor, M., Landmann, R. (2009). Furanone at subinhibitory concentrations enhances staphylococcal biofilm formation by luxS repression. *Antimicrobial Agents Chemotherapy*, 53, 4159–4166. doi:10.1128/AAC.01704-08

Maguire, R., Duggan, O., Kavanagh K. (2016). Evaluation of *Galleria mellonella* larvae as an in vivo model for assessing the relative toxicity of food preservative agents. *Cell Bioogy Toxicology*, 32, 209–216. doi:10.1007/s10565-016-9329-x.

Megaw, J., Thompson, T. P., Lafferty, R. A., Gilmore, B. F. (2015). *Galleria mellonella* as a novel in vivo model for assessment of the toxicity of 1-alkyl-3-methylimidazolium chloride ionic liquids, *Chemosphere*, 139, 197–201. doi:10.1016/j.chemosphere.2015.06.026

Otto, M. (2012) Molecular basis of *Staphylococcus epidermidis* infections. *Semin. Immunopathol.* 34, 201–214. doi:10.1007/s00281-011-0296-2.

Pankey G. A. & Sabath, L. D. (2014). Clinical Relevance of Bacteriostatic versus Bactericidal Mechanisms of Action in the Treatment of Gram-Positive Bacterial Infections, *Clinical Infectious Disease*, 38, 864–870. doi:10.1086/381972

Rasmussen L., White, E. L., Pathak, A., Ayala, J. C., Wang, H., J.-H. Wu, Benitez, J. A., Silva, A. J. (2011). A high-throughput screening assay for inhibitors of bacterial motility identifies a novel inhibitor of the Na<sup>+</sup>-driven flagellar motor and virulence gene expression in *Vibrio cholerae*. *Antimicrobial Agents Chemotherapy*, 55, 4134–43.

doi:10.1128/AAC.00482-11

Sardi, J. C. O., Freires, I. A., Lazarini, J. G., Infante, J., Alencar, S. M., Rosalen, P. L. (2017). Unexplored endemic fruit species from Brazil: Antibiofilm properties, insights into mode of action, and systemic toxicity of four *Eugenia* spp. *Microbial Pathogenesis*, 105, 280–287. doi:10.1016/j.micpath.2017.02.044

Trentin, D. S., Giordani, R. B., Zimmer, K. R., Silva, A. G., Silva, M. V., Correia, M. T. S., Baumvol, I. J. R., Macedo, A. J. (2011). Potential of medicinal plants from the Brazilian semi-arid region (Caatinga) against *Staphylococcus epidermidis* planktonic and biofilm lifestyles. *Journal of Ethnopharmacology*, 137, 327–335. doi:10.1016/j.jep.2011.05.030

Trentin, D. S., Silva, D. B. Amaral, M.W., Zimmer, K.R., Silva, M. V, Lopes, N.P., Giordani, R.B., Macedo, A.J. (2013). Tannins Possessing Bacteriostatic Effect Impair *Pseudomonas aeruginosa* Adhesion and Biofilm Formation. *Plos One*, 8, e66257. doi:10.1371/journal.pone.0066257

Trentin, D. S., Silva, D. B., Frasson, A. P., Rzhepishevskaya, O., Silva, M. V., Pulcini, E. L., James, G., Soares G. V., Tasca, T., Ramstedt, M., Giordani, R. B., Lopes, N.P., Macedo, A. J. (2015). Natural Green coating inhibits adhesion of clinically important bacteria. *Scientific Reports*, Feb 6;5:8287. doi: 10.1038/srep08287

Van Horn, K. S., Burda, W. N., Fleeman, R., Shaw, L.N., Manetsch, R. (2014). Antibacterial activity of a series of N2,N4-disubstituted quinazoline-2,4-diamines. *Journal of Medicinal Chemistry*, 57, 3075–3093. doi:10.1021/jm5000408

Van Horn, K.S., Zhu, X., Pandharkar, T., Yang, S., Vesely, Vanaerschot, B., Dujardin, M. J.-C., Rijal, S., Kyle, D. E., Wang, M. Z., Werbovetz, K.A., Manetsch, R. (2014). Antileishmanial activity of a series of N 2,N 4-disubstituted quinazoline-2,4-diamines, *Journal Medicinal Chemistry*, 57, 5141–5156. doi:10.1021/jm5000408

VanEpps, J. S. & Younger, J. G (2016). Implantable Device-Related Infection,

*Shock*, 46(6), 597–608. <https://doi.org/10.1097/SHK.0000000000000692>

Wang, Q., Sun, F.J., Liu, Y., Xiong, L. R., Xie, L. L., Xia, P. Y. (2010). Enhancement of biofilm formation by subinhibitory concentrations of macrolides in icaA/BC-positive and -negative clinical isolates of *Staphylococcus epidermidis*. *Antimicrobial Agents Chemotherapy*, 54, 2707–2711. doi:10.1128/AAC.01565-09

Zhang, Q., Nguyen, T., McMichael, M., Velu, S. E., Zou, J., Zhou, X., Wu, H. (2015). New small-molecule inhibitors of dihydrofolate reductase inhibit *Streptococcus mutans*. *International Journal Antimicrobial Agents*, 46, 174–82. doi:10.1016/j.ijantimicag.2015.03.015